JOURNAL OF MATERIALS SCIENCE **35** (2000) 4207–4213

The creep behaviour of Synroc and alumina

E. G. MEHRTENS, K. U. SNOWDEN
Materials Division, Australian Nuclear Science and Technology Organisation, Private Mailbag 1, Menai, NSW 2234, Australia
E-mail: egm@ansto.gov.au

The creep of Synroc C and alumina in four-point bending in argon was investigated in terms of the relaxed symmetric stress and the reference asymmetric stress; the alumina being used as a reference material. The creep tests were undertaken in the temperature range from 850°C to 1300°C. The rupture behaviour of Synroc at 950°C indicated a high stress exponent, and that the creep ductility was unusual in that the strain increased with increasing test time. A scanning electron miscroscopy examination of Synroc after creep revealed the development of defect-free oxidised surface layers. For Synroc, neither prior exposure to pre-heating in air, nor prior indentation affected the creep rate behaviour. This was attributed to the formation of the oxidised surface layers and the associated "healing" effects of the damage produced by the indentations.

1. Introduction

Access to basic creep information is important in assessing the design, manufacture and performance of ceramics exposed to high temperatures during fabrication or service [1, 2]. In contrast to the extensive literature on the creep of alumina, there appears to be no creep data available in the case of Synroc C, which is a ceramic designed to immobilise the radioactive elements in high-level nuclear waste. In determining creep properties, investigators have shown a preference for bending creep tests over uniaxial creep tests because of the difficulties of accurate alignment, gripping, and temperature uniformity required for the latter method [3]. However, one problem with the bending creep of ceramics is that the neutral axis is not generally located at the centre of the beam but is displaced towards the compression surface of the beam [3, 4]. This may arise from the creep resistance in compression being different from that in tension and can result in differences in creep behaviour when bending and uniaxial data are plotted in terms of the maximum principal stress. Jakus and Wiederhorn [5] have proposed that the estimated values of strain can be considered an "average" of the surface strains. While the displacement of the neutral axis and the subsequent stress redistribution have been analysed in detail [6–10] the analyses have proved to be fairly complex and difficult to use [11]. Recently Dyson and Gibbons [3] have introduced a relatively simple geometry-dependent "reference stress" which was shown to correlate the bending and uniaxial creep data for silicon nitride at 1204 and 1300°C.

The present work reports the results of four-point bend creep tests on Synroc C and alumina at elevated temperatures to provide creep data and in the case of alumina to compare the present results with those published in the literature. The reference stress was used in conjunction with the symmetric relaxed stress to analyse the results of the bending creep tests.

2. Materials and experimental methods

Synroc C is a multi-phase ceramic designed to immobilise the radioactive elements in high-level nuclear waste (HLW) [12]. It has an approximate solidus temperature of 1600 K and the following nominal composition (wt %): 57.0 TiO_2, 5.4 ZrO_2, 4.3 Al_2O_3, 4.4 BaO, 8.9 CaO and 20.0 HLW. Hot pressing was undertaken in a graphite die in which Synroc C powder together with simulated HLW was contained within an iron capsule which was separated from the die wall by a layer of Synroc powder. A pressure of 20 MPa was maintained for 3 h at 1230°C after which the material was cooled to 300°C in about 20 h. The density was 4.35×10^3 kg/m^3. Specimens were prepared from hot-pressed Synroc C cylindrical blocks 80.5 mm diameter by 25 or 80 mm thick. Specimen blanks were sliced from the blocks using a 2 mm thick diamond saw, then polished to provide a standard smooth surface using silicon carbide papers (120 grit to 1200 grit), and finished on 0–0.25 μm diamond paste to remove all visible machining marks and surface defects; the specimen edges were bevelled using the same polishing techniques.

For the alumina samples, commercially available alumina of 99.7% purity was used. It had an average grain size of 3–4 μm, a hardness of 17 GPa and a density of 3.90×10^3 kgm/m^3. The material was supplied in the form of sintered flat bars approximately 50 mm long, 8 mm wide and 2 mm thick. The bars as-supplied had a good surface finish with a surface roughness of approximately 0.6 μm.

All specimens were tested in the as-received condition execpt for those tests in which the specimens were subjected to prior heating or prior indentation.

The alumina and Synroc C specimen dimensions were approximately $8 \times 2 \times 50$ mm or $8 \times 4 \times 50$ mm. The specimens were measured before testing in four-point bending under load control conditions, in an Instron 8561 Universal testing machine. The four-point bending jig manufactured from silicon nitride had spans of 20×40 mm (load pins rotating) which is consistent with the ASTM C 1161 (1990) configuration B [13]. The specimen deflection was measured directly with a displacement transducer attached to an alumina rod with a silicon nitride tip in contact with the centre of the specimen on the tension side. The four-point bending creep tests covered temperatures in the range of 850 to 1300°C. The extent of the deflection of the specimen during creep was limited by the bending jig, which allowed a maximum deflection of 4 mm (or a maximum strain of about 4% for the 2 mm thick specimens and about 7% for the 4 mm thick specimens).

The time, load, deflection and ram position test parameters were automatically captured and stored via an A-D board to a computer. The time between readings could be set depending on the expected length of the test; an interval of between 1 and 100 seconds was usually chosen. The total number of points for each test was typically between 150 and 2,000 with a maximum of 4,000.

The tests were undertaken in a split "Severn" furnace in dynamic argon atmospheres, which were used in an attempt to reduce the effects of possible oxygen contamination of specimens. Although no information was available on Synroc, environmental effects on the mechanical properties of alumina and other ceramics have been reported elsewhere [14, 15]. The spaces around the pull rods were plugged with "Kao wool", and high purity argon ($O_2 < 10$ ppm, $N_2 < 50$ ppm) was fed into the furnace at a steady rate of 15 litres/minute. The specimens were held at temperature for approximately 30 minutes before testing to allow all components to come to equilibrium.

The stresses and strains for four point bending were calculated using the methods given below.

3. Stress and strain analysis

Two possible models for stress and strain were considered: where the neutral axis is at the centre of the beam (symmetric), and where the neutral axis is displaced towards the compression surface of the beam (asymmetric).

3.1. Symmetric bending stress

The creep tests in four-point bending were undertaken by setting the testing machine in load control and maintaining the load (P) constant in order to give a symmetric maximum elastic fibre stress of

$$\sigma_{\text{el}} = \frac{3Pa}{2bh^2} \tag{1}$$

where a is the inner span, h is the thickness and b the width.

For symmetric bending the neutral axis is located at the centre of the beam.

3.2. Relaxed symmetric stress

Creep data are usually plotted in terms of Hollenberg *et al.*'s [16] relaxed symmetric stress, σ_{sym}, for four-point bending.

$$\sigma_{\text{sym}} = \sigma_{\text{el}}\left(\frac{(2n+1)}{3n}\right) \tag{2}$$

where n is the stress exponent in the Norton equation $\dot{\varepsilon} \propto \sigma^n$. This assumes that sufficient time has elapsed for the initial maximum elastic stress to creep down to the above value. Robertson *et al.* estimate this time for alumina at 1250°C to be "a few minutes" [17].

3.3. Symmetric elastic strain

The elastic strain for two beam geometries were considered. These were when: (i) the beam geometry is an arc of a circle between the two inner support points (Fig. 1), and (ii) the beam geometry is an arc of a circle between the two inner loading points and stress redistribution occurs by creep.

(i) Timoshenko [18] gives the elastic deflection of a beam in four-point bending at the centre (y_c) as:

$$y_c = \frac{P}{48EI}(L-a)\{3L^2 - (L-a)^2\} \tag{3}$$

where I is the moment of inertia and E is the elastic modulus. Taking $\varepsilon_{\max} = \frac{\sigma_{\max}}{E}$, $\sigma_{\max} = \frac{Mh}{2I}$ and $M = \frac{P(L-a)}{2}$, where M is the bending moment about the neutral axis, in Equation 3 gives

$$\varepsilon_{\max} = \frac{12hy_c}{2L^2 + 2aL - a^2} \tag{4}$$

which is the same expression as that given by Munz and Fett [19].

(ii) The expression relating the centre deflection (y_c) and the outer fibre strain has been derived by the authors [20] using a method similar to that of Hollenberg *et al.*, except that Hollenberg *et al.* solved for (y_L)

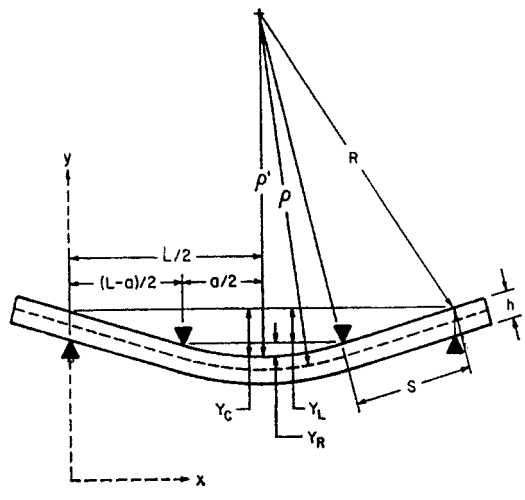

Figure 1 The geometry of the partly circular bent beam, after Hollenberg *et al.* [16].

whereas in the present work the solution is for (y_c). The strain at the centre of the beam (ε_c) is

$$\varepsilon_c = \frac{hy_c}{\left(\frac{n}{n+2}\right)\left(\frac{L-a}{2}\right)^2 - \frac{L^2}{4}} \quad (5)$$

Equation 5 reduces to Equation 4 when $n = 1$.

3.4. Asymmetric bending

The creep strains (above eqs.) estimated from curvature data, have assumed that the neutral axis is at the centre of the beam. For ceramic materials, the creep strength in compression is not usually equal to that in tension and this can lead to a shift of the neutral axis from the centre of the beam towards the compressive surface.

Recently Dyson and Gibbons [3] have treated the bending stress for creep rupture in terms of a reference stress (σ_{ref}) given by

$$\sigma_{ref} = \frac{1}{6}\sigma_{el}\left[\frac{(2n+1)}{n}\right]^{n/(n+1)} \quad (6)$$

This equation was shown to be valid for hot pressed silicon nitride at 1204°C and 1300°C in that rupture data from bend and compression tests were in agreement when the bend test data were plotted in terms of σ_{ref} and the compression data in terms of the principal axial stress. The times to rupture (t_f) are governed by events at the skeletal points provided

$$\lambda > \left|\frac{\sigma_{ref}}{\sigma_{el}}\right| \quad (7)$$

where

$$\lambda = \frac{\varepsilon_f}{\dot{\varepsilon}.t_f} \quad (8)$$

and ε_f is the fracture strain, and t_f is the time to fracture.

4. Results and discussion

The creep properties of Synroc C and alumina in four-point bending have been evaluated in terms of the relaxed symmetric stress and the reference asymmetric stress. The use of the relaxed stress has been widely used to express bending creep data, whereas the more recently introduced reference stress has the advantage that bending creep test results can be related to those of uniaxial creep tests.

Fifty eight creep tests were completed, 48 on Synroc C and 10 on alumina. In addition, 6 Synroc specimens were tested under non-standard conditions in which the specimens were subjected to prior heating or prior indentation (see Section 4.3 below). Scanning electron microscopy was undertaken on four Synroc specimens after creep testing.

4.1. The stress dependencies of the creep rates of Synroc and alumina

The stress dependencies of the secondary creep rate for Synroc and alumina are given for the relaxed and/or reference stresses in the Figs 2–4. The creep rates were taken after the transitions from a primary to a secondary creep stage in a creep rate versus time plot as described by Lin and Becher [21]. The Synroc results at 950°C suggested that the stress dependence increased from $n = 1.6$ to a higher value of about 10 at a stress of $\sigma_{sym} \approx 110$ MPa.

An Oak Ridge group has given alumina results for both bending and compression creep tests [22]. Their

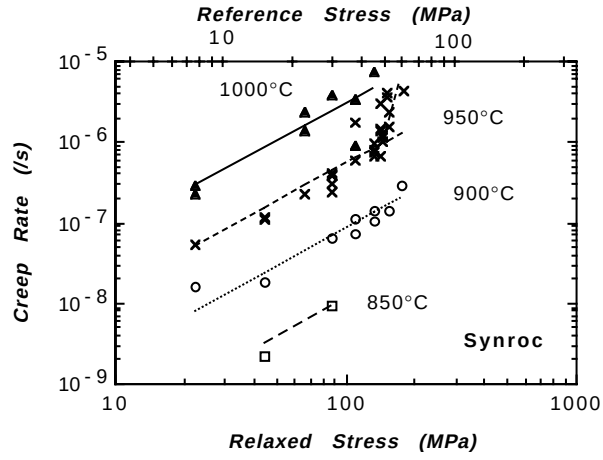

Figure 2 Creep rate versus the relaxed and the reference stresses for Synroc C under flexural loading. The lines are the fits to the Norton equation, Equation 9.

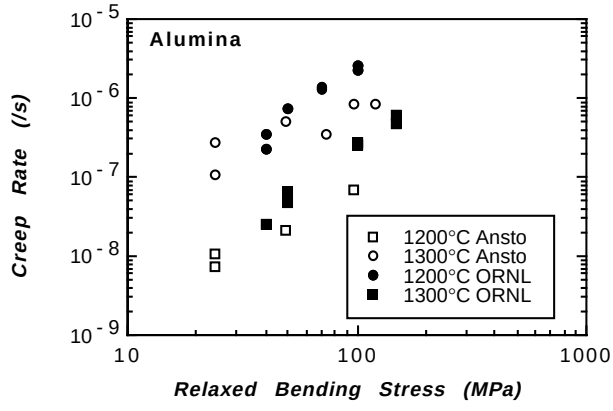

Figure 3 Creep rate versus elastic stress data for ORNL (reference [22]) and ANSTO aluminas under flexural loading.

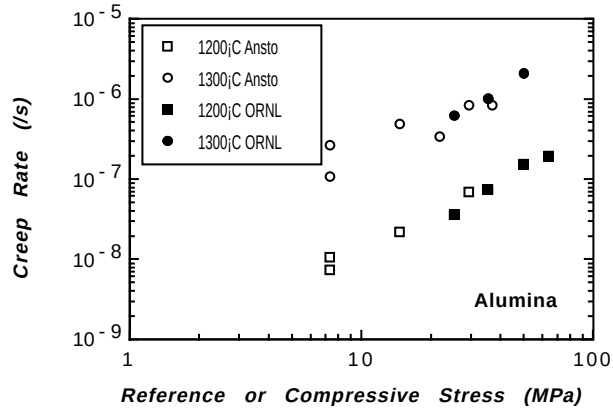

Figure 4 Creep rate versus compressive and reference stresses curves for ORNL (reference [22]) and ANSTO aluminas.

bending results are compared with the present data in Fig. 3 and these show some agreement, particularly at the lower stresses. However, the Oak Ridge data have a higher stress exponent, $n \approx 2.3$, compared that of the present results, $n \approx 1.2$, see below. The Oak Ridge compression results were compared with the present results plotted in Fig. 4 as a function of the reference stress, σ_{ref}, given by Equation 6. Fig. 4 shows that the present reference bending-stress data were in reasonable agreement with the axial compression-stress (maximum principal) data obtained by Salem and Choi [22] for material tested at 1200°C and 1300°C.

The creep rate data were fitted by regression analysis to a Norton type equation of the form:

$$\dot{\varepsilon} = A\sigma^n \exp\left(\frac{-Q}{RT}\right) \tag{9}$$

With the creep rate based on Equation 9, that is, $\dot{\varepsilon} = \dot{\varepsilon}_c$, the stress given by Equation 2, that is $\sigma = \sigma_{sym}$, and for $\sigma_{sym} < 110$ MPa (because of the change of slope at about this stress). The regression analysis gave:

For Synroc, $n = 1.56(\pm 0.14)$, $A = 3.168 \times 10^9$, and $Q = 443(\pm 22)$ kJ/mol. (Correlation coefficient: $R^2 = 0.948$).

For alumina, $n = 1.17(\pm 0.23)$, $A = 3.313 \times 10^9$ and $Q = 531(\pm 56)$ kJ/mol. (Correlation coefficient: $R^2 = 0.954$).

The figures in parenthesis indicate ± the Standard Error. With the reference stress based on Equation 6, that is, $\sigma = \sigma_{ref}$, and the creep rate based on Equation 5 as before, the regression analysis gave:- $A = 1.685 \times 10^{10}$ for Synroc, and $A = 6.929 \times 10^9$ for alumina and the same values of the other parameters.

As noted above, no known creep data for Synroc were available for comparison, however, Sherby and Miller [23] have found that, for a range of materials, the stress for a given strain rate is primarily a function of the corresponding elastic modulus and more recently Raj [1] has pointed out that the lattice diffusion coefficient often correlates with the elastic bulk modulus. If Synroc C conforms to this latter correlation, then taking the elastic modulus as 161 GPa (as measured on the present material), the activation energy for lattice diffusion is about 460 kJ/mol, which is comparable to the above value for creep (443 ± 22 kJ/mol).

For alumina, the present data are in general agreement with the results of creep tests reported by Heuer *et al.* [24] Robertson *et al.* [17] and by the Oak Ridge group [21, 22, 25] who report stress exponents of about n from 1.1 to 2 and activation energies of 390 and 568 kJ/mol. The values of $n \approx 1$ to 2 were suggested to arise from grain-boundary sliding. Robertson *et al.* reported the activation energies at the lower end of the above range and suggested the diffusion of oxygen and Al in alumina [26] is controlling creep mechanism. However, more recent work by Le Gall *et al.* has indicated a higher value (510 kJ/mol) for Al in alumina single crystals [27] which is closer to the value obtained in the present work. Calderon-Moreno *et al.* [28] point out that while grain boundary sliding is the generally accepted mechanism in this general stress and temperature range, the nature of this sliding, that is whether interface-reaction or transport of matter controlled, appears to depend on the grain size dependence of the creep rate, something which was not investigated in the present work.

4.2. The creep rupture behaviour of Synroc

Only four Synroc creep rupture results at 950°C were obtained at $\sigma_{sym} > 150$ MPa because of the jig limitations mentioned above. These data are given as log (rupture life) versus log(stress) in Fig. 5a for both the relaxed and reference stresses. Results for two specimens tested to longer times without failure are also given. The Figure suggests a stress exponent of $m \approx 12.4$, where m is given by $t_f \propto \sigma^{-m}$. The value of m may be in accord with the suggested higher value of n at stresses > 110 MPa. The four ruptured Synroc specimens conformed to the inequality given by Equation 7.

Fig. 5b gives the rupture strain or final strain results as a function of test time at 950°C. The Figure indicates that, despite only four rupture results being obtained, there is a clear indication that when taken together with the other non-rupture test results, the creep strain increases with test time. This time dependence of the rupture strain is the opposite to that found with many materials [29, 30] and appears to be related to the formation of a defect-free oxide layer at both the compression and tension surfaces.

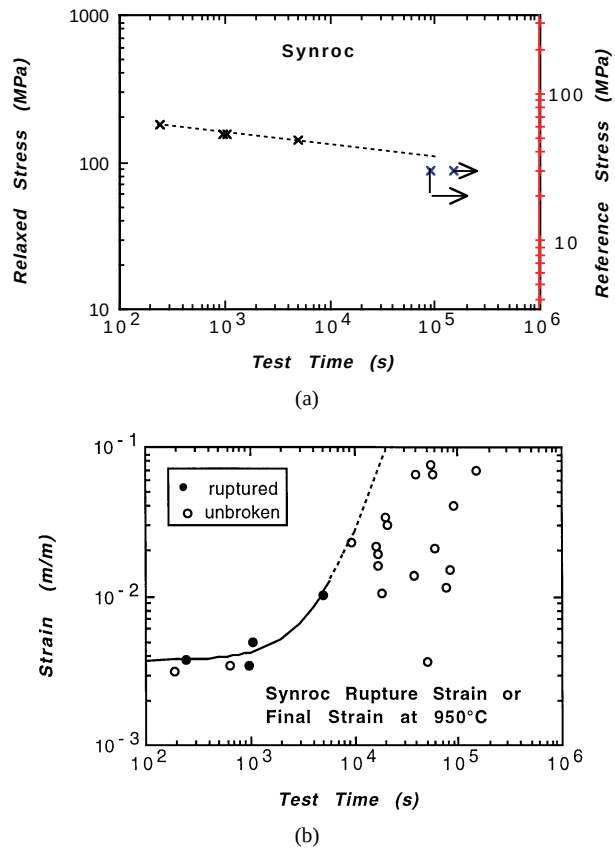

Figure 5 (a) The Synroc creep rupture results at 950°C. Arrows indicate unbroken specimens. (b) The Synroc creep rupture and final creep strain, ε_c, results versus test time at 950°C.

4.3. Pre-exposed and indented Synroc

Six tests on Synroc specimens were undertaken with non-standard conditions, these were:

- Two tests, which were made on specimens pre-heated in air at 1000°C for 4 h prior to creep testing at 950°C in argon in the standard way; and
- Four specimens, which were each subjected to three 20 kg Vickers hardness indentations (one at the centre of the beam and one 5 mm either side of the centre) at room temperature prior to creep testing at 950°C in argon in the standard way.

The former two tests were undertaken to determine if prior exposure to air at elevated temperature influenced the subsequent creep behaviour in argon, while the latter four tests were performed to examine if pre-existing cracks might lead to an accelerated creep rate with possible premature failure. The creep rate results for the non-standard specimens are compared with those for the standard specimens in Fig. 6.

These creep rate results indicate that, at 950°C, neither prior heating at 1000°C nor prior indentation had a significant influence on the creep rate.

The specimens subjected to prior exposure to heating in air for 4 h at 1000°C apparently had the formation of the oxidised surface layers enhanced without affecting the creep rate. Similarly, the formation of the oxidised layers on the specimens given prior indentations would tend to "heal" the cracks and the damage associated with the indentations. This is supported by constant stress-rate tests on indented Synroc specimens tested in bending in argon at 900°C, where the fracture stress increased with decreasing stress rate or increasing time to failure [31]. Choi and Tikare [32] have discussed three possible crack healing mechanisms: bond restoration of clean fracture surfaces, reaction with the environment resulting in new phases across the crack plane, and transport of existing phases across the crack plane. All three mechanisms could have played a role in the healing of the indented Synroc specimens. However, while the latter two mechanisms appear more likely, there was no way of discriminating between the mechanisms as creep tests in a good vacuum were not possible with the present apparatus.

4.4. Microstructure of Synroc C

The present creep tests were undertaken in a dynamic environment of argon to reduce the possible effects of the ambient air atmosphere on the results. Nevertheless after creep, the microstructure of Synroc C revealed that oxidised surface-regions had formed at both the tension and compression surfaces in the form of a surface oxidised layer and a modified structural layer. Fig. 7 shows a scanning electron micrograph of a section which is typical of the original Synroc C microstructure consisting of titanate phases, hollandite + zirconolite + perovskite + titanium oxides and/or minor calcium-aluminum titanates, plus small amounts of metallic alloys and a calcium-rich phosphate (see reference [12] for details). Fig. 8a illustrates a scanning electron micrograph of a through-thickness section near the tension surface of a specimen which had been subjected to creep for 15 h at 950°C and had sustained a strain of $\varepsilon_c = 7.6\%$ without failure. No detectable grain boundary- or transgranular-cracking was found either in the oxidised or the modified structural layers, or the adjoining centre region. Fig. 8b shows the oxidised surface layer and the modified structural layer at higher magnification. Fig. 8c shows the transition region between the modified structural layer and the un-modified central region. The oxidised layer was approximately 25 μm thick and the adjoining deeper modified structural layer was approximately 170 μm thick. The modified structural layers appeared to have formed by the loss of metallics from the surface region leaving a small amount of micro-porosity with pore size ≤ 2 μm. The oxidised surface layers appeared to have resulted from recrystallisation and the loss of micro-porosity from the near surface modified structural region. A scanning electron microscopy examination of other specimens after creep testing for periods of 0.3 h to 14 h at 950°C also showed no evidence of cracking and indicated that the thicknesses of both the oxidised surface layer and the modified structural layer increased with increasing time at temperature and tended to level off

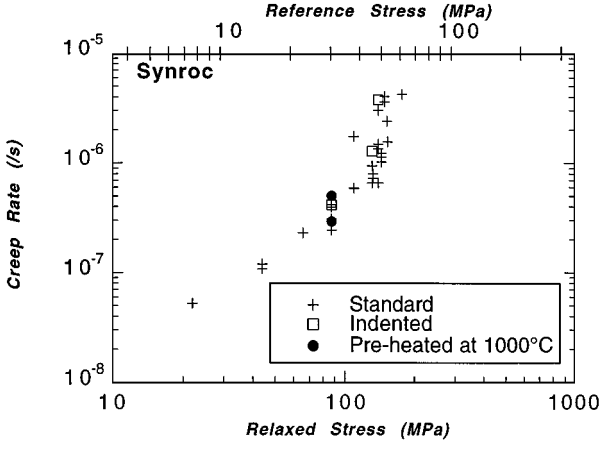

Figure 6 The stress dependence of the creep rate at 950°C of the standard Synroc specimens and the creep rates of pre-heated and indented specimens.

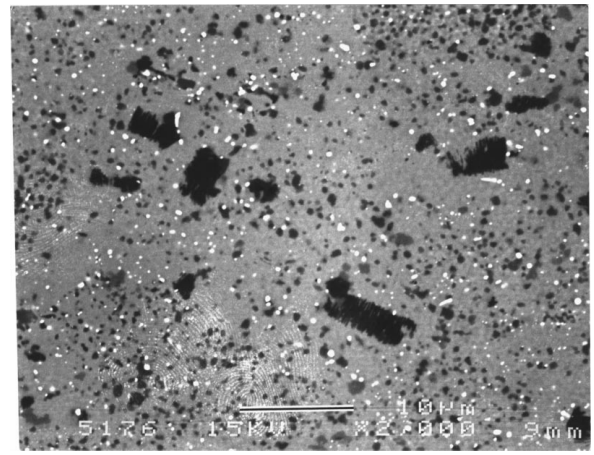

Figure 7 A SEM micrograph of Synroc showing an area which is typical of the original structure. The bar represents 10 μm.

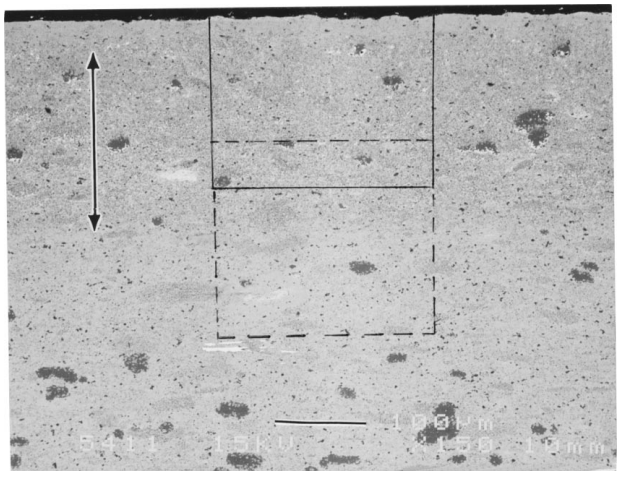

(a)

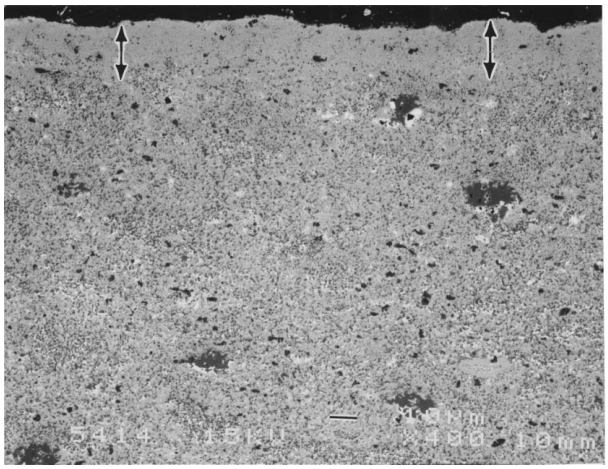

(b)

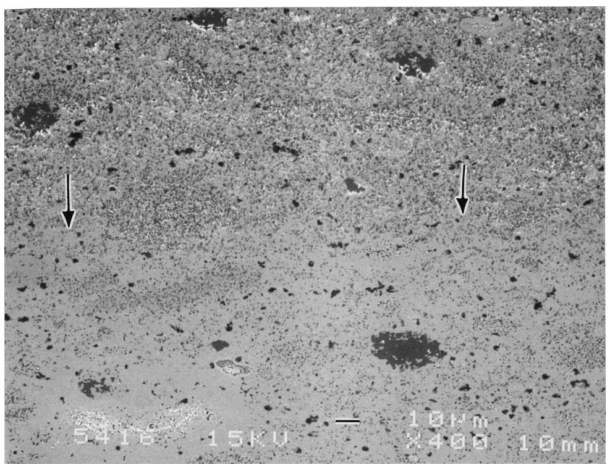

(c)

Figure 8 (a) The tension surface region after creep for 15 h at 950°C and a strain of $\varepsilon_c = 7.6\%$ without failure . The double headed arrow indicates the extent of the modified structural layer. The bar represents 100 μm. The marked areas indicate the regions shown in Fig. 8b and c. (b) The surface area marked in Fig. 8a at higher magnification. The double headed arrows indicate the extent of the oxidised surface layer. The bar represents 10 μm. (c) The transition region shown in Fig. 8a at higher magnification. The arrows indicate the approximate depth of the modified structural layer. The bar represents 10 μm.

after ≈5 h which suggested that the surface layers were protective.

A through-thickness section of a specimen exposed to air at 1000°C for 4 h prior to being creep tested at 950°C for 13.7 h to a strain of $\varepsilon_c = 2.1\%$ without failure showed the presence of oxidised surface layers similar to those of the standard specimens, however, the thickness of the modified structural layers were approximately twice that of the standard specimens. This suggested that the high temperature exposure prior to creep testing affected the size of the modified structural layer but had little influence on the size of the oxidised surface layer. The similarity in the creep behaviour of the prior oxidised specimens to that of the standard specimens (Fig. 6) suggests that it is the oxidised surface layers, rather than the modified structural layers, which determine the creep strength.

5. Conclusions

- The creep behaviour of Synroc C and alumina in four-point bending in a dynamic test atmosphere of argon was investigated in terms of the relaxed symmetric stress (σ_{sym}) and the reference asymmetric stress (σ_{ref}). The creep data were fitted to a Norton creep rate equation using both these stresses. Regression analysis gave:-

  From 48 Synroc creep tests at 25 to 150 MPa and 850°C to 1000°C, for $\sigma_{sym} < 110$ MPa $n = 1.56(\pm 0.14)$, and $Q = 443(\pm 22)$ kJ/mol. (Correlation coefficient: $R^2 = 0.948$).

  From ten alumina creep tests at 25 to 125 MPa and 1200°C and 1300°C, $n = 1.17(\pm 0.23)$ and $Q = 531(\pm 56)$ kJ/mol. (Correlation coefficient: $R^2 = 0.954$).

- The creep rupture behaviour of Synroc at 950°C and $\sigma_{sym} > 150$ MPa indicated a high stress exponent $m \approx 12$ where the rupture life is given by $t_f \propto \sigma^{-m}$. The creep ductility of Synroc at 950°C was unusual in that the rupture strain or final strain increased with increasing test time.
- Microstructural examination using SEM of Synroc after creep testing revealed the development of defect-free oxidised layers ≈30 μm thick at the compression and tension surfaces; this was despite the tests being undertaken in a dynamic atmosphere of argon.
- For Synroc, neither prior pre-heating in air at 1000°C for 4 h, nor prior indentation using a 20 kg load affected the subsequent creep rate behaviour in argon. This was attributed to the formation of the defect-free oxidised surface layers and the "healing" effects of the cracks and damage produced by the indentations.
- The most appropriate stress for creep tests in bending appears to be Dyson and Gibbons' reference stress (σ_{ref}) in that, for alumina, the reference stresses, which were derived from the bending stresses, were reasonably consistent with uniaxial stresses (Fig. 4).
- It is useful to give Hollenberg *et al.*'s relaxed symmetric stress (σ_{sym}) for comparison purposes, because other investigators have used this stress.

Acknowledgements

The authors wish to thank Mr P. Angel for fabricating the Synroc samples, Mr S. Leung for his assistance with the electron microscopy, Messrs F. van Luyt and K. McKay for machining the specimens, Messrs J. Warmeant and T. Nicholls for polishing the specimens and Mr R. P. Harrison for helpful comments on the manuscript.

References

1. R. RAJ, *J. Am. Ceram. Soc.* **76** (1993) 2147.
2. Y. S. KWON, G. SON, J. SUH and K. T. KIM, *ibid.* **77** (1994) 3137.
3. B. F. DYSON and T. B. GIBBONS, *Materials Science and Technology* **9** (1993) 151.
4. M. K. FERBER, M. G. JENKINS and V. J. TENNERY, *Ceram. Eng. Sci. Proc.* **11** (1990) 1028.
5. K. JAKUS and S. M. WEIDERHORN, *J. Amer. Ceram. Soc.* **71** (1988) 832.
6. T. J. CHUANG, *J. Mater. Sci.* **21** (1986) 165.
7. C. F. CHEN and T. J. CHUANG, *J. Amer. Ceram. Soc.* **73** (1990) 2366.
8. T. FETT, K. KELLER, M. MISSBACH and D. MUNZ, *ibid.* **71** (1988) 1046.
9. T. FETT, K. KELLER and D. MUNZ, *J. Mater. Sci.* **23** (1988) 467.
10. T. FETT, M. MISSACH and D. MUNZ, *J. European Ceram. Soc.* **13** (1994) 197.
11. G. D. QUINN and R. MORRELL, *J. Amer. Ceram. Soc.* **74** (1991) 2037.
12. A. E. RINGWOOD, S. E. KESSON, K. D. REEVE, D. M. LEVINS and E. J. RAMM, "Synroc, in Radioactive Waste Forms for The Future," edited by W. Lutze and R. C. Ewing (Elsevier Science Publishers B. V., 1988) p. 233.
13. ANONYMOUS, ASTM Standard, ASTMC 1161-90, p. 327, and p. 847.
14. SUNG R. CHOI, VEENA TIKARE and J. A. SALEM, *Scripta Met. et Mater.* **29** (1993) 189.
15. GUEN CHOI and SUSUMU HORIBE, *J. Mater. Sci.* **30** (1995) 1565.
16. G. W. HOLLENBERG, G. R. TERWILLIGER and R. S. GORDON, *J. Amer. Ceram. Soc.* **54** (1971) 196.
17. A. G. ROBERTSON, D. S. WILKINSON and C. H. CACERES, *ibid.* **74** (1991) 915.
18. S. TIMOSHENKO, in "Strength of Materials Pt 1" (Van Nostrand Coy., Princeton, NJ, 1955) p. 159.
19. D. MUNZ and T. FETT, "Mechanshes Verhalten Keramisher Werkstoffe" (Springer-Verlag, Berlin, 1989) p. 181.
20. K. U. SNOWDEN and E. G. MEHRTENS, *J. Mater. Sci. Letters* **16** (1997) 278.
21. H.-T. LIN and P. F. BECHER, *J. Am. Ceram. Soc.* **73** (1990) 1378.
22. J. A. SALEM and S. R. CHOI, ORNL/TM-11984, March 1992, p. 305–319.
23. O. D. SHERBY and A. K. MILLER, *J. of Eng. Mater. and Tech.* **101** (1979) 387.
24. A. H. HEUER, N. J. TIGHE and R. M. CANNON, *J. Am. Ceram. Soc.* **63** (1980) 53.
25. H. T. LIN, P. F. BECHER and W. H. WARWICK, ORNL-11984, 1992, pp. 265–267.
26. A. M. BROWN and M. F. ASHBY, *Acta Metall.* **28** (1980) 1085.
27. M. LE GALL, B. LESAGE and J. BERNARDINI, *Plil. Mag.* **70** (1994) 761.
28. J. M. CALDERON-MORENO, A. R. DE ARELLANO-LOPEZ, A. DOMINGUEZ-RODRIGUEZ and J. L. ROUTBORT, *J. European Ceramic Soc.* **15** (1995) 983.
29. B. R. LAWN, A. G. EVANS and D. B. MARSHALL, *J. Amer. Ceram. Soc.* **63** (1980) 574.
30. T. DARROUDI and R. A. LANDY, *Amer. Ceram. Soc. Bull.* **66** (1987) 1139.
31. E. G. MEHRTENS and K. U. SNOWDEN, unpublished work, 1992.
32. S. R. CHOI and V. TIKARE, *Mater. Sci. and Eng.* **A171** (1993) 77.

Received 24 April 1997
and accepted 19 January 2000